2016

Laser control of electron matter waves

Eric Jones
University of Nebraska-Lincoln

Maria Becker
University of Nebraska-Lincoln, mgbecker3@gmail.com

Jom Luiten
Eindhoven University of Technology

Herman Batelaan
University of Nebraska-Lincoln, hbatelaan@unl.edu

Published in *Laser Photonics Rev.* 10:2 (2016), pp. 214–229. doi 10.1002/lpor.201500232

Submitted 17 September 2015; revised 18 January 2016; accepted 28 January 2016; published online 2 March 2016.

Laser control of electron matter waves

Eric Jones,[1] Maria Becker,[1] Jom Luiten,[2] and Herman Batelaan [1]

1 Department of Physics and Astronomy, University of Nebraska—Lincoln, 208 Jorgensen Hall, Lincoln, Nebraska 68588-0299, USA
2 Department of Applied Physics, Eindhoven University of Technology (TU/e), P.O. Box 513, 5600 MB, Eindhoven, The Netherlands

Corresponding author — H. Batelaan, email hbatelaan2@unl.edu

Abstract
In recent years laser light has been used to control the motion of electron waves. Electrons can now be diffracted by standing waves of light. Laser light in the vicinity of nanostructures is used to affect free electrons, for example, femto-second and atto-second laser-induced electrons are emitted from nanotips delivering coherent fast electron sources. Optical control of dispersion of the emitted electron waves, and optically controlled femto-second switches for ultrafast electron detection are proposed. The first steps towards electron accelerators and matter optics on-a-chip are now being taken. New research fields are driven by these new technologies. One example is the optical generation of electron pulses on-demand and quantum degenerate pulses. Another is the emerging development of interaction free electron microscopy. This review will focus on the field of free electron quantum optics with technologies at the interplay of lasers, electron matter waves, and nanostructures. Questions that motivate their development will also be addressed.

Keywords: electron, femto-second, nanostructure, microscopy, laser

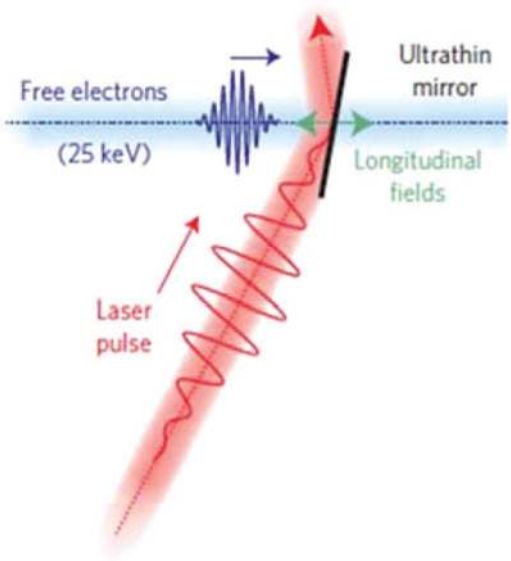

1. Introduction

How much radiation damage do low-energy resonances impart to humans? [1] Can charged particle radiation therapy be made more cost-effective? [2, 3] The answers to such questions have societal impact. How will movies of protein folding and other biological processes be made? [4,5]. Can the electron trajectory in a double-slit experiment be tracked? [6] Answers to these questions can deepen our understanding to long standing scientific problems. Can the coupling between gravity and electromagnetism be observed? [7–9] Is the Pauli exclusion principle a symmetry or a consequence of dynamics? [10,11] These questions are speculative and their relevance is unclear, but considering them may lead to changes in our fundamental description of nature.

Such questions appear unrelated, however, recent developments in free electron quantum optics (FEQO) on coupling between laser light, free electrons and nanostructures may lead to technologies that can address the above questions. Electrons can now be diffracted by standing waves of light [12]. Laser light in the vicinity of nanostructures is used to affect free electrons, for example, femto-second [13,14] and atto-second [15] laser-induced electrons are emitted from nanotips delivering coherent fast electron sources. Optical control of dispersion of the emitted electron waves [16], and optically controlled femto-second switches for ultrafast electron detection [17] are proposed. The first steps towards electron accelerators and matter optics on-a-chip are now being taken [18]. New research fields are driven by these new technologies. One example is the optical generation of electron pulses on-demand and quantum degenerate pulses [19]. Another is the emerging development of interaction free electron microscopy [20, 21]. This review will focus on the field of free electron quantum optics [22] with technologies at the interplay of lasers, electron matter waves, and nanostructures, that may address the questions raised above. For example, laser-based charged particle accelerators built on a chip may be used for radiation therapy. Time-of-flight techniques may lead to the indentification of low-energy electron resonances. Ultrafast electron diffraction can be used to make movies of protein folding. Weak measurements may allow for the tracking of electron trajectories. Dynamics of electron degeneracy may probe the onset of the Pauli exclusion principle. To be able to give somewhat more detailed answers to these questions we now turn our attention to the technological developments that allow us to consider these questions.

In 1933, Kapitza and Dirac estimated that a mercury arc lamp, the strongest known laboratory light source at the time, would deflect one in every 10^{14} electrons [23]. Consequently,

attempts to measure this so-called Kapitza-Dirac effect started only after the development of the laser. In 1988 Bucksbaum demonstrated high-laser intensity deflection of electrons, which marks the first observation of the manipulation of free electron motion with laser light [24]. Electrons were deflected by ponderomotive potential gradients, and a description with classical mechanics gave good agreement with the data. In 2001, the first manipulation of quantum motion of electrons by laser light was observed as diffraction of electrons by a standing wave of light [12]. This is the Kapitza-Dirac effect. This effect provides a coherent beamsplitter for electrons, similar in function to a piece of glass or a grating for a light beam.

The Kapitza-Dirac experiment was partly inspired by the many successful experiments in atom optics, where atomic motion was controlled with laser light [25], and many applications of such techniques, including Rubidiumbased atomic clocks used in the Global Positioning System [20]. Electrons in atoms can be manipulated with laser light at lowintensities as the light is tuned to the electron resonant transitions. Free electrons have no such resonances and higher intensities must be used. A Q-switched, one Joule laser pulse of 10 ns was used to give a pulsed electron diffraction pattern, synchronous with the laser pulse, in the observation of the Kapitza-Dirac effect. Two properties of the realization of the Kapitza-Dirac effect, its coherence and its pulsed nature, could have applications in electron diffraction and interferometry (using coherence) or electron time-of-flight measurements (using pulses). However, the combined use of pulsed lasers with CW electron beams resulted in a low duty cycle and low count rate of 0.1 e^{-}/s. This is an obstacle for making useful devices.

Two approaches can be followed to overcome this obstacle. First, the laser-light standing wave grating can be replaced with a nano-fabricated grating [26]. This results in higher count rates at the expense of losing timing. In the last decade, nano-fabrication of electron optics elements has evolved to create free-standing structures, which now includes free-standing double slits [27] and spiral phase plates [28]. Forked gratings have been developed, which are used to produce high quality electron Laguerre Gaussian beams [29]. Electron interferometers with man-made gratings, as opposed to naturally occurring crystals, have also been realized [30–33].

The second approach to overcome low count rates is the use of an on-demand electron source of sufficient coherence. This allows for timing of all electrons in such a way that they can interact with a second, appropriately timed laser pulse, such that coincidence techniques are not necessary and the count rate can increase dramatically. A pivotal experiment in 2006 operated a field emission tip in combination with a femto-second laser [13]. The result was an on-demand high repetition, high brightness, femto-second electron source [14, 34].

For the purpose of developing a femto-second resolution electron time-of-flight apparatus, the tip can act as a start, but a stop is needed too. Femto-second resolution electron detection is thus needed. Streaking by synchronizing RF-cavities with the electron pulses has been used for this purpose [35]. The use of laser light to illuminate nanofabricated structures and create near-fields that affect the motion of nearby free electrons has been proposed [17]. Yet an additional element is needed to make a time-of flight device. Electrons emitted from the emission tip have a velocity spread that increases the electron pulse width upon propagation. This dispersion must be undone to retain femto-second resolution. RF-compressors are now commercially available to deliver 100 femto-second pulses on a target [36]. Pulsed laser compressors [16, 37] and a continuousfield dispersion compensator [38] have also been proposed to reach the atto-second domain. Alternatively, electrons can be extracted from laser cooled atoms to give very low dispersion electron sources [39] that may not require control of dispersion.

The field emission tip is the electron source of choice in electron microscopy [40]. By applying a DC voltage to a nanometer size tip, electric fields are created that cause electrons to tunnel into the vacuum. The field of a tightly focussed laser from a femto-second oscillator gives comparable fields and leads to a femto-second electron pulse that is synchronous with a femto-second laser pulse. The nanometer scale of the tip leads to relatively large coherence lengths for electron waves emitted from the tip [41–43].

The logical combination of a femto-second coherent electron pulse with a second femto-second laser pulse has been pioneered in Zewail's group [44, 45], and recently led to the observation of standing plasmon waves in a nanoneedle [46]. Nobel laureate Ahmed Zewail also pioneered femto-chemistry, which led to ultrafast electron diffraction and ultrafast electron microscopy [47]. One of the first applications of ultrafast electron diffraction that involved both nanometer and femto-second resolution, was a study of an ultrafast, laser-induced, solid-liquid phase transition in polycrystalline aluminum [48]. Recently, Ropers first implemented a transmission ultrafast low energy electron diffraction (T-ULEED) with a field emission tip, resolving dynamics in a polymer/graphene bilayer at picosecond timescales [49, 50].

Pulsed electron microscopy can yield so many electrons in one nanosecond pulse, that in a single shot a complete image can be recorded. This technique has been developed by the Livermore DTEM (dynamic transmission electron microscopy) group [51–53]. The electron sources often used in pulsed electron microscopes are often photocathodes that are typically fast, but tens of microns in size, leading to a limited coherence length, which limits the applicability to small size structures (atoms, molecules). Femto-second tip sources extend the range and the type of electron microscopes as for example in ultrafast TEM [54]. Femto-second single-electron pulses with the coherence properties of field emission tips may also be produced by chopping the beam in an electron microscope with an RF cavity [55].

A 4 keV electron passing over a 100 nm periodicity nanofabricated grating passes adjacent bars in a time of 2.7 femtoseconds. This matches the period of a 800 nm laser and thus gives the possibility of manipulating electron motion with the electric field of the laser. The grating acts as a rectifier. In comparison, the KD-effect is not due to the electric field of the laser

directly, but due to the time averaged Lorentz force, and thus a weaker effect. Periodic arrays have been made that show plasmonic enhancement of the near-fields [56], so that even lower laser intensity could be used. One of the most exciting developments along these lines are near-field electron accelerators on a chip [2, 57].

In electron microscopy, a challenge is imaging biological samples with high resolution without changing them by electron exposure. It would be a remarkable feat if interaction free measurement could be used to create an electron microscope that produces images with virtually no electron exposure. This is the goal of recent work at Stanford, MIT, Delft and Erlangen [20, 21]. At Stanford the KD-effect is used to split an electron beam, which is captured in a recycling electron trapwith twoweakly coupled arms.Asample placed in one arm can stop the coherent evolution of electrons into that arm, which leads to detection of the sample without exposure.

All of the above discussion concerns one-electron physics. Multi-electron pulses have also been generated [34]. This leads to the question, can degenerate electron pulses be made in free space? The highest reported electron degeneracy in free space is about 10^{-4} in a measurement of the Hanbury Brown-Twiss effect [22]. This unique electron quantum optics experiment may point theway to a newtype of quantum degenerate electron beam. The electron source used was a continuous field emission tip. Replacing it with a femto-second laser controlled emission tip is expected to lead to much higher degeneracies [19]. Multi-electron pulses from tips could thus be used to further open the field of electron quantum optics. In summary, the combination of laser light to manipulate electrons in free space, with or without nano-structures, leads to many new scientific and technological avenues to explore, and can be called free electron quantum optics (FEQO).

2. The Kapitza-Dirac effect

Consider an electron placed initially at rest in a standing wave of light. The vector potential can be given by, $A_z = A_0 \cos kx \sin \omega t$. The electric and magnetic fields are

$$E_z = -\frac{\partial}{\partial t} Az = -A_0\, \omega \cos kx \cos \omega t$$
$$B_y = -\frac{\partial}{\partial x} Az = A_0\, k \sin kx \sin \omega t \qquad (1)$$

The electric field is $\pi/2$ out of phase with the magnetic field in space and time. If the electron is located halfway between a maximum and a zero crossing in the electric field ($x = \lambda/8$), then it will be accelerated by the electric field along the z-axis. The resulting electron velocity $v_z = 1/m\, eA_0 \cos(kx) \sin(\omega t)$ lags behind by a phase of $\pi/2$ with respect to the electric field. The electron's velocity will lead to a Lorentz force, $F_x = -ev_z B_y$. As a result, the electron oscillates in phase with the magnetic field, and a time-averaged Lorentz force is found [58]. This force can be expressed in terms of the ponderomotive potential,

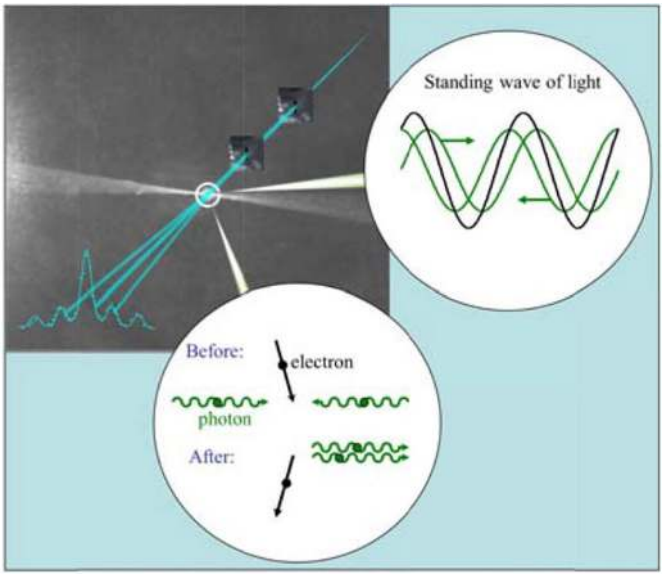

Figure 1. Kapitza-Dirac effect. A schematic of an electron matter wave (blue, from top right to left bottom) diffracted by a laser beam illustrates the role reversal of matter and light in the particle-wave duality.

$$V_p = \frac{e^2 A_0^2}{4m} \cos^2 kx = \frac{e^2 I}{2m\varepsilon_0 c\omega^2} \cos^2 kx \qquad (2)$$

This potential can be inserted in the Schrödinger equation to yield diffraction peaks with transverse momenta $2\hbar k$ and diffraction peak strengths given by $|dm|^2 = J_m^2(V_0 t/\hbar)$ [59]. Alternatively we can think of the potential writing a phase grating on an electron plane wave, whence the momentum distribution can be obtained by Fourier transform. This is indeed what is found experimentally [12] (see Fig. 1). The blue solid line is a solution to the Schrödinger equation that matches the experimental data (blue points) well.

A frequency doubled 50 Hz, 532 nm Q-switched laser of 0.1 J energy and 10 ns pulse duration was used. The electron diffraction pattern was thus pulsed synchronously with the laser light. From the resolved diffraction peaks it is clear that several standing wave nodes were coherently illuminated by the electron beam. The transverse coherence length is estimated to be 0.5–1 micrometers, and the count rate is 0.1 e/s.

3. The matter optics analogy, nano-fabricated gratings and vortices

In the Kapitza-Dirac effect the electron plays the role of the wave and light plays the role of the grating in a role reversal as compared to the usual light diffraction from a material grating. This type of wave-partice duality is a part of the matter optics analogy and motivates switching out material components with shaped and modulated laser beams. This interplay can go back and forth.

Instead of a laser standing wave providing a phase grating for the electron, a nanofabricated grating can be used to provide an absorption grating [26, 60]. The fact that this can be done is based on the fact that the time-dependent Schrödinger equation can be rewritten, when the potential V in the Schrödinger equation does not depend on time, as the time-independent Schrödinger equation,

$$\nabla^2\phi + \frac{2\,(E-V)}{m\hbar^2}\phi = 0 \tag{3}$$

Defining the factor $2(E-V)/m\hbar^2$ as k^2 gives the Helmholtz equation,

$$\nabla^2\phi + k^2\phi = 0 \tag{4}$$

the solutions of which also describe the steady state solutions for optics. This well-known analogy is a defining property of the field of matter-optics. For a material grating with a periodicity of 100 nm and an electron energy of 900 eV, highly resolved diffraction peaks can be obtained. The diffracted orders retain their coherence as they can be recombined and interfere in near-field [32,33] and far-field interferometers [30]. Double slits have been ion-milled to realize Feynman's thought experiment [61], including the closing and opening of the individual slits [33]. Gratings have been modified to produce angular momentum electron Laguerre-Gaussian modes, [28] which have also been combined into electron microscopes [62]. Electron vortex beams that resemble atomic orbitals have been produced, which could be used for magnetic mapping with atomic resolution in electron microscopy [63]. Ion-milling of forked gratings has been the key to this development [29]. The diffracted electron beam orders can carry up to to 100 $\hbar$ of angular momentum (Fig. 2).

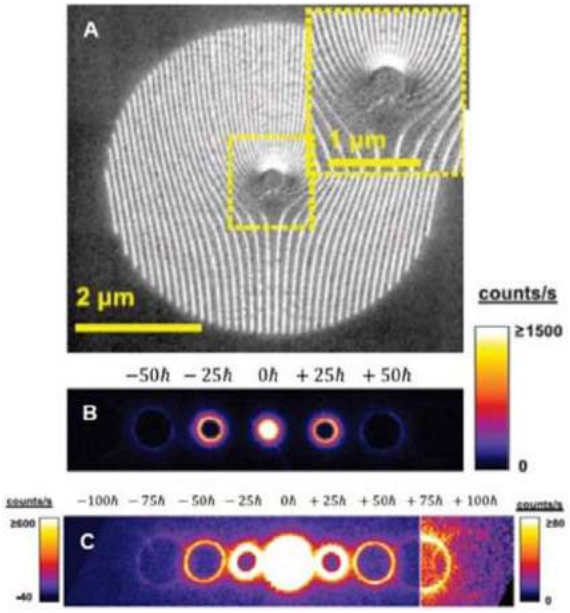

Figure 2. Nanofabricated diffraction grating with fork dislocations (A) are used to produce multiple diffracted electron vortex beams (B and C). The fork dislocation, magnified in the inset of (A), is defined by b additional half-slits in the grating pattern. The grating shown in (A) has a periodicity of 100 nm and dislocation number b = 25. Diffraction patterns produced when a 300 keV spatially coherent electron beam is transmitted through the grating are shown in (B) and (C). Each ring-shaped spot is the transverse intensity profile of an electron vortex beam; the corresponding orbital angular momenta, L_z , are indicated. The third and fourth diffraction orders, with L_z = 75$\hbar$ and L_z = 100$\hbar$ respectively, can be seen on the right in (C) where a different color scale has been applied. The figure is modified from McMorran et al. 2011 (reference [29]).

Reversing the matter-optics analogy back again, an alloptical method for producing electron vortex modes has been proposed (Fig. 3) [64]. The idea uses Kapitza-Dirac scattering of electrons with circularly polarized light carrying $\pm l\hbar$ orbital angular momentum. As a result of conservation of orbital angular momentum the diffracted electron orders will have $+2nl\hbar$ units of orbital angular momentum. There are several advantages of using laser light to manipulate coherent electrons. Materials in the vicinity of electron beams can remove coherence, due to for example image charge interaction. With laser light interaction there is no decoherence. Laser light can be shaped in situ and one can switch from regular standing waves to forked standing waves. This could lead to the capability in transmission electron miscoscopy (TEM) to switch between regular images to spiral phase microscopy in TEM [65] to enhance edge visibility [62].

4. On-demand electron sources and double slits-in-time

In 2006, a field-emission tip was combined with a femto-second laser, providing a high repetition rate femto-second electron source [34,66] (Fig. 4 left). This technique is an alternative to photocathode sources,which with the latest developments still provide competitive parameters [67]. For field-emission tips, a tungsten tip of tens of nanometers diameter is illuminated with a focussed 800 nm femto-second laser pulse having nanojoule energy. Several mechanisms can cause electron emission [68]. Field-emission can cause tunnelling from the Fermi level. Multiphoton emission gives enough energy to overcome the work function. Above threshold ionization adds additional photon energy to the electron's motion, while photo-emission involves one-photon absorption followed by tunnelling. Ropers [69] showed tunneling at high bias voltage and multiphoton electron emission at low bias for gold and tungsten nanotips, and explored the transition from quiver motion to strong field emission from tips through a range of wavelengths [70]. Most of these processes give an electron emission rate that is non-linear in the laser intensity. This is fortunate as it can be used to place an upper bound on the electron pulse duration. When two femto-second pulses illuminate the tip with a time delay between them, the electron count rate is the sum of both pulses individually only when the pulses are not overlapping and the first pulse does not affect the electron emission of the

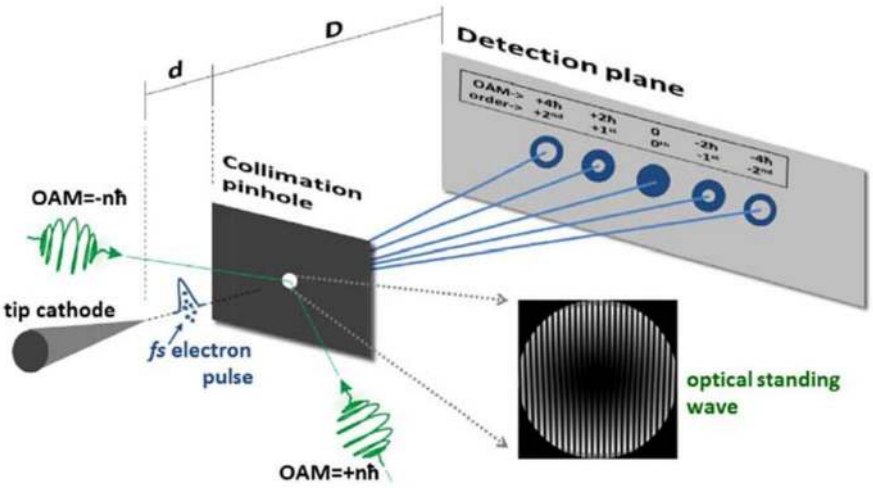

Figure 3. An all optical method for producing electron vortex modes. A femto-second electron pulse generated at a tip cathode travels a distance *d* to a pinhole. Two femto-second laser pulses create an optical standing wave with a fork dislocation. The Laguerre-Gaussian or "donut" laser modes transfer orbital angular momentum to the electron as it diffracts from the standing wave. The electrons travel a distance *D* to the detection plane, where the diffracted electrons themselves show the "donut" spatial distribution. The figure is modified from Handali et al. 2015 (reference [64]).

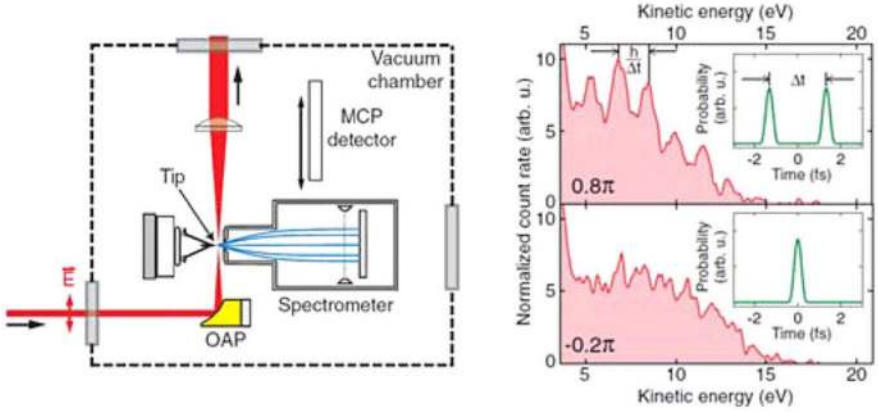

Figure 4. Double slit-in-time. Left: A tungsten tip is illuminated with a CEP controlled femto-second laser pulse to extract electrons. The energy spectrum of the electron is measured with a spectrometer. Right: The energy spectrum of the electron double pulses shows distinct peaks with a separation in energy that is the reciprocal of the electron pulse separation in time (top). For a single electron pulse the peaks are mostly removed (bottom). The figure is modified from Krüger et al. 2012 (reference [68]).

second pulse [66]. This was shown experimentally [14] and establishes that the electron source acts at the femto-second scale.

More recently, methods were developed to control the electron emission with the instantaneous field of electromagnetic waves. Photoemission from a nanotip was gated by the presence of a single-cycle terahertz pulse delayed with respect to a 800 nm 50 fs pulse [71]. Carrier envelope phase (CEP) control was used to demonstrate that the electron emission can be limited to a single or double laser cycle [15,68]. This latter case will now be discussed in some detail. The single pulse arises when the maximum of the laser pulse envelope coincides with a field maximum. The highly non-linear emission process causes the field maximum to generate one dominant electron pulse. If the laser pulse envelope straddles the adjacent field maxima then an electron double pulse is generated. This gives rise to double slit-in-time [72–75] and demonstrates the coherence of electron pulses separated in time down to the atto-second domain (Fig. 4 right) [68]. This is a remarkable experimental demonstration of the analogous more familiar double slit-in-space, [27] and another example of a matter-optics analogue.

To understand double-slit diffraction-in-time, one can take the Fourier transfrom of the spectrum to obtain the energy spectrum. Alternatively, consider an analogy to the usual diffraction in space. Two coherent sources separated in space by Δx give rise to a comb of momenta separated by $\Delta p_x = \hbar/\Delta x$. The spatial pattern measured at the detector, placed at a distance L from the sources, will show a comb of maxima separated by $L\Delta p_x/p$. Analogously, two coherent sources separated in time by Δt give rise to a comb of energies separated by $\Delta E = \hbar/\Delta t$. The temporal pattern, measured at the detector as a function of time t, has a comb with maxima separated by $t\Delta E/2E$. If instead the kinetic energy difference between the sources, $\Delta E_{kin} = E(t - \Delta t) - E(t)$, is considered, a beat period is found $T_{beat} = h/\Delta E_{kin}$ that is identical to the spacing of the temporal pattern, $t\Delta E/2E$. The result can thus be interpreted as a beat note between two electron waves with different energy, just as the spatial diffraction pattern can be interpreted as an interference between two electron waves with different momenta. In the experiment performed by Hommelhoff [15,68], the beat note in time is not measured, which makes the analogy to spatial double slit diffraction less direct. Instead, the single slit and double slit energy distributions are measured. The spatial equivalent would be to measure the single slit and double slit transverse momentum distribution. While the single slit in time distribution of Fig. 4 does not show prominent peaks, and the double slit distribution does, it can be inferred that there is interference between the two slits and

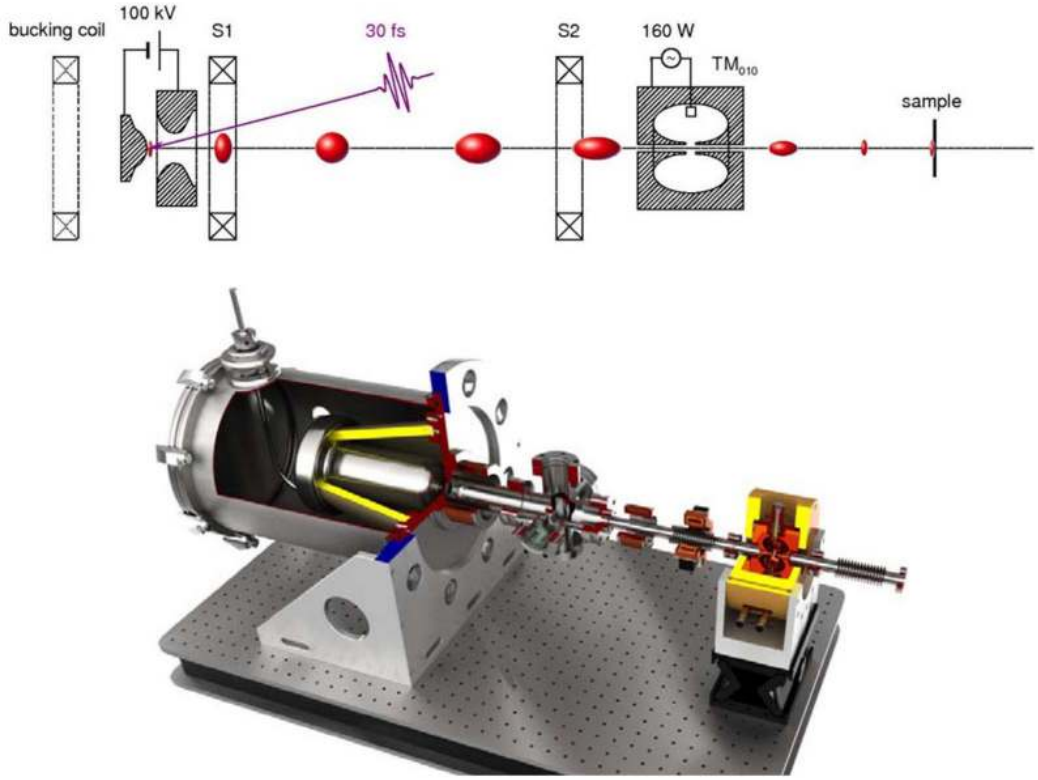

Figure 5. RF compression [81]. Top: Ellipsoidal electron bunches are generated by photoemission with femto-second laser pulses (left) and the electron bunches are focused in the transverse (magnetic coils) and longitudinal (microwave cavity) direction on the target (right); Bottom: the ultrafast electron diffraction (UED) setup. The figure is modified from Luiten et al. 2015 (reference [81]).

thus diffraction. Diffraction-in-time has also been experimentally demonstrated so far for chopped atomic beams [76], cold neutrons [77], and above-threshold ionization of argon [78].

5. Pulse compression

Laser induced electrons emitted from an emission tip have an energy and velocity spread. Consequently, the fast electrons will pull ahead of the slow electrons, and this dispersion broadens the electron pulse quickly. A technique is required to deliver the pulsed electrons with high temporal resolution on a target. An RF compressor that delivers 100 fs electron pulses synchronously with a laser pulse on a target was proposed in 2007 [35] and is now commercially available [36,79]. Figure 5 shows the schematic and design of the device, that for 100 keV and 0.2 pC electron pulses, demonstrates microwave bunch compression from 10 ps to 100 fs. This technique has been applied to ultrafast electron compression [80].

Temporal lensing has also been proposed as a method to compensate for the dispersion of electron pulses [16]. This optical technique uses appropriately timed laser pulses to intercept electrons as they propagate though free space. The laser pulse acts as a lens to focus the electron packet in the time domain through the ponderomotive force. Both RF compression and electron pulse compression with laser beams are based on the same idea. An oscillating field is timed so that fast electrons that arrive at the compressor first encounter a field that slows them down, and slow electrons that arrive later encounter a field that speeds them up. Some distance of propagation after the compressor the electrons bunch up to a short pulse. Because the interaction is time-dependent, the compressed pulse can be shorter than the initial pulse. The trade-off is that the compressor needs to be precisely timed to intercept the electron pulse.

Alternatively, one can build an electron dispersion compensator. The idea [38] is similar to the optical dispersion compensator. Electrons of different velocities are spread to parallel trajectories. The fast electrons follow longer trajectories so that they exit the dispersion compensator after the slow electrons. Upon free propagation, the electrons again reform a pulse (Fig. 6). As the interaction is timeindependent, the reformed pulse can only be as short as the incident pulse. The advantage is that no timing is required. Acomparable elegant idea is compression based on an electrostatic mirror [82]. The α-Spherical Deflector Analyzer (α-SDA) utilizes a spherically symmetric capacitor cavity in an arrangement similar to spherical energy analyzers already in use in electron microscope applications [82–84]. The outer shell of the cavity is kept at a negative voltage, while the inner shell is kept at a positive voltage, and the radius is chosen to match the geometric orbits of electrons for a fixed energy. Fast electrons in a pulse entering the α-SDA will take a longer orbit, and experience deceleration by the negative shell of the

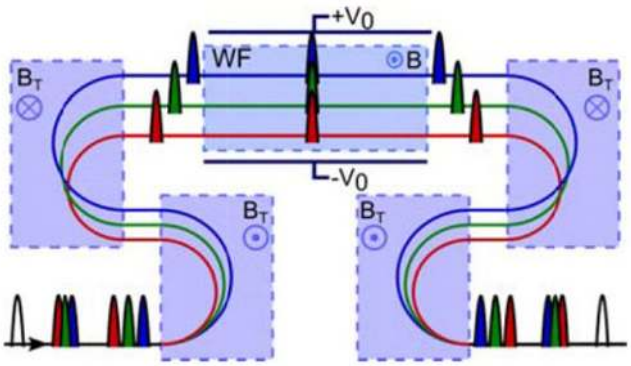

Figure 6. Electron Dispersion Compensator (EDC) [38]. An electron pulse is generated and disperses (left bottom). The electrons are spatially dispersed with two uniform magnetic fields (B_T) in proportion to their kinetic energy. Higher (lower) energy electrons are indicated in blue (red). A Wien filter (WF) compensates the relative delay between the electrons. The WF is set so that the action of the deflectors plates at a potential V_0 is balanced by the magnetic field B. The electrons are recombined by two further magnetic fields (right bottom). The figure is taken from Hansen et al. 2012 (reference [38]).

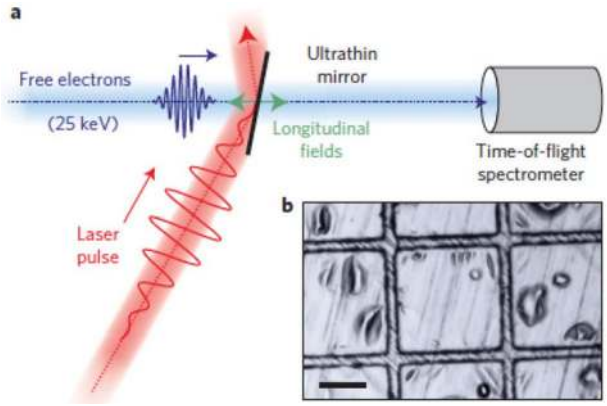

Figure 7. Laser streaking of free electron pulses. a) Electrons (blue) pass through an thin metal mirror (black). A laser pulse (red) passes through the electron pulse at an angle. Because the laser propagation direction is angled with respect to the electron velocity (green), the electron experiences parallel and antiparallel laser fields components. The electrons are pushed out of the field in less than half an optical cycle. The streak camera has thus a resolution given by the field oscillations. b) Image of the freestanding aluminium film with a thickness of 50 nm. Scale bar, 100 mm. The figure is taken from Kirchner et al. 2014 (reference [94]).

device. Slow electrons take a shorter orbit, and are accelerated by the positive shell. The electrons temporally overlap briefly when they have made a half orbit through the α-SDA, but they are spatially defocused. The effect of a pulse completing an orbit through the device is the mirror-symmetric reversal of fast and slow electrons comprising the pulse, thus the device acts as a transparent electron mirror.

A new exciting development is that electrons can be extracted with a femto-second laser pulse from laser cooled atoms to give very low dispersion electron sources [39] that may not require control of dispersion.

6. Fast detection

Use of these pulse compression techniques requires the ability to accurately measure the temporal characteristics of ultrashort pulses. Streaking is currently the method of choice for fast detection. Electrons pass through an oscillating magnetic field produced in an RF cavity [36, 55, 85]. The integrated field the electrons experience while travelling through the cavity deflects the electrons sideways. The deflection is dependent on the RF phase and thus the time that the electrons arrive at the cavity. For a series of times, the electrons sweep across a detector screen. A position dependent detector is used to measure the streak pattern on the screen, and thus the temporal profile of the electrons.

One can also devise a means by which to use a laser pulse as a switch. Low power optical electron switches have already been realized [86]. Electron beams are deflected up to 1.2 mrad when they pass by a silicon-nitride surface that is illuminated by a low-power, continuous-wave laser. The suggested mechanism for this effect is that the laser beam causes a redistribution of charges on the surface, which sets up a field capable of deflecting the electrons. The moderate temporal response of this switch was found to be 6 μs. Applications may include electron lithography and electron microscopy.

A laser could be used to intercept the free electrons without a structure present, and its ponderomotive potential could be used to deflect the beam. With two counterpropagating laser beams, a femto-second version of the Kapitza-Dirac effect has been realized, and by changing the delay between the laser and electron pulse, the pulse duration can be measured [87].

Observation of electron motion in atomic systems has been a longstanding goal of ultrafast electron diffraction. Interesting targets in which to study this behavior have already been proposed [88, 89]. This type of sub-atomic four-dimensional imaging requires atto-second temporal resolution. Electron pulses at tens of keV with de Broglie wavelengths of 1–10 pm have been used in ultrafast electron diffraction to provide picometer resolution [90–93]. The temporal resolution of such electron pulses is of the order of several hundred femto-seconds, and is limited by space-charge effects in multi-electron pulses. Use of these techniques requires the ability to accurately measure the temporal characteristics of compressed pulses. Recently, laser streaking has been demonstrated by Kirchner [94] as a method for achieving this with potentially subfemto-second resolution.

The technique of Kirchner et al. for atto-second streaking of freely propagating electron pulses is based on the atto-second streak camera concept. An electron pulse and a laser pulse intersect at an ultrathin metal mirror as shown in Fig. 7. The mirror consists of a freestanding aluminum film that is transparent to the electrons, but reflective for the laser pulse. The electrons experience laser fields parallel and antiparallel to their propagation

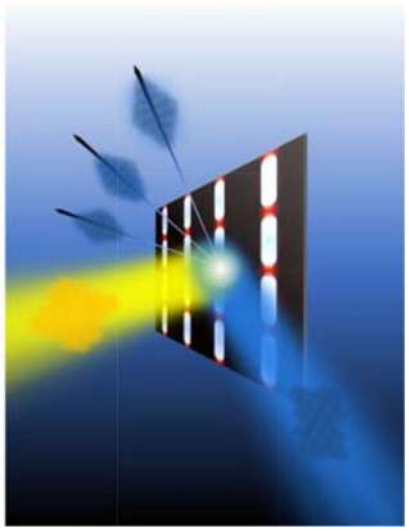

Figure 8. Coherent femto-second electron switch. An electron pulse (blue) passes through the enhanced near field (red) of a plasmonic antenna. A laser pulse (yellow, synchronous with the electron pulse) affects the electron motion by the ponderomotive potential, i.e., the same interaction responsible for the Kapitza- Dirac effect. Following Zewail [96], the electron velocity vector can remain synchronous with the laser pulse as they sweep over the planar plasmonic structure. The temporal resolution of the switched and coherent electron beams (outgoing blue lines) is the laser pulse duration. The figure is taken from Becker et al. 2013 (reference [17]).

direction because of the noncollinear geometry of the two pulses. The penetration depth of these laser fields into the mirror is subwavelength due to the nanoscale thickness of the structure.

As a result, electrons pass through the laser fields in less than half of an optical cycle. The field amplitude gives rise to an energy gain of the electrons, which depends on their arrival time at the mirror. Appropriate tuning of the angles of incidence and use of phase-controlled laser pulses enable this scheme to function as an atto-second streak camera for ultrafast electron pulses. The electron pulse is effectively stretched longitudinally, making time-of-flight spectrometry feasible for temporal characterization. Kirchner, et al. demonstrated their technique with 25 keV electron pulses and 50 fs streaking laser pulses at a wavelength of 800 nm and peak intensity of ~0.4 TW cm^{-2}. The free-standing aluminum foil mirror had a thickness of 50 nm. The passage of the electrons through the field occured within 200 as. With a time-of-flight spectrometer providing a resolution of ~1 eV, the electron pulse duration was determined to be 360+/-20 fs. This proof-of-principle measurement is expected to be transferrable to subfemto-second electron pulses. Simulations conducted in this regime indicate that streaking spectroscopy can serve as a method for temporal characterization of such ultrashort electron pulses, including their pulse shape, duration, bandwidth, chirp and coherence.

The use of near-field enhancing plasmonic antennas has been proposed to measure the pulse duration of a coherent electron pulse, while using low intensity lasers [17]. This type of structure could be used as an ultrafast switch for electrons (Fig. 8), as it has been shown to have a temporal response faster than 20 fs. The enhanced near-fields, which result when resonant femtosecond laser pulses are incident on the structure, may be capable of deflecting passing electrons by up to tens of mrad. Spatially resolved electron detectors used in combination with this type of ultrafast electron switch could be used to characterize the temporal properties of electron pulses. Another possible application of such an ultrafast electron switch is ultrafast electron microscopy, which is widely used to study chemical and physical processes on short temporal and spatial scales [95].

Another technique for fast switching has been proposed that uses the interaction of a laser beam with a nanofabricated dielectric photonic structure to deflect free charged particles. Switching speeds of less than a femto-second are predicted. This method is discussed in detail in section 8 [97].

The interaction of laser pulses with materials is also used to switch optical pulses. Slow light photonic crystals are used to switch optical pulses, which propagate through the material. Absorption of a femto-second pulse modulates the refractive index, which redirects the optical pulse. This type of switching has been shown to have a temporal resolution of 3 ps [98].

7. PINEM and seeing plasmons

Having a synchronous electron and laser pulse, where both can be directed onto a structure, raises another question. Can energy be delivered to an electron by the laser light if they simultaneously pass near the structure? The context of this question is provided by the long standing debate on whether or not an electron can be accelerated by a laser field. Although the Lawson-Woodward theorem [99] indicates that electrons can not be accelerated by laser light, it has been shown that energy gain by laser interaction is possible for high-energy electrons directed through an intense tight laser focus [24].But can it be done for low-energy electrons with moderate laser intensity? The answer is affirmative in the presence of nanostructures. Garc´ıa de Abajo first developed the concept of electrons passing by an excited plasmonic structure to image the near fields [100–102]. This “PINEM” technique [45], pioneered experimentally in Zewail’s group, which recently demonstrated simultaneously the imaging of standing plasmon waves in silver nanowires and the energy they exchanged with femto-second electron pulses, is an example of the control of electron energy (Fig. 9) [46].

A near-IR laser pulse is used to heat or excite a target. A second pulse, split off and delayed from the first, is focused onto an electron source to generate ultrashort electron pulses. The target evolution can then be observed in real time, by changing the delay between the electron imaging pulse and laser excitation pulse. In vacuum a single photon cannot interact with free electrons as this violates energy– momentum conservation [59]. In comparison, spontaneous Compton scattering involves two photons of different frequency. The Kapitza-Dirac effect is stimulated Compton scattering that allows two-pho-

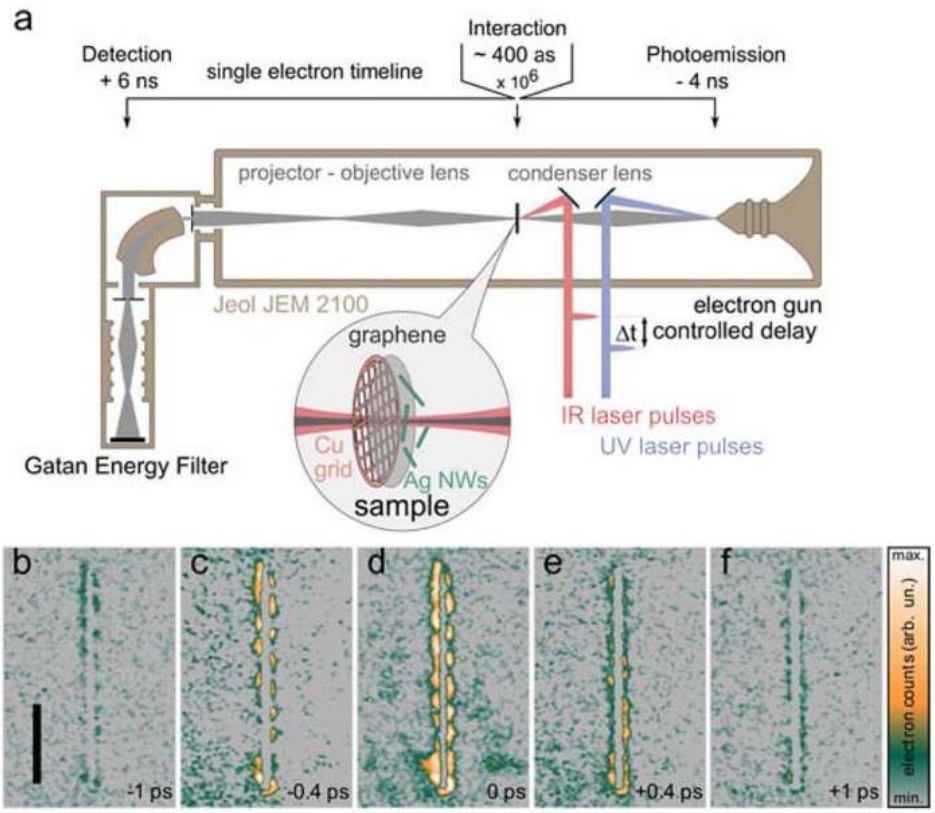

Figure 9. PINEM schematic. Ultrashort electron pulses, containing no more than a single electron per pulse, are generated from a LaB_6 tip and directed toward a sample of Ag nanowires (5.7 μm length, 67 nm radius) supported by a graphene mesh. The nanowires are accessible to focused 800 nm fs laser light with polarization control and time delay relative to the electron pulses. The laser light photoexcites surface plasmon polaritons (SPPs) on the nanowires, which are then probed by the passing electron pulses. The electron pulses can experience discrete energy shift in units of $\pm\hbar\omega$ = ±1.55 eV after interaction with the SPP near-fields. Images of the spatial pattern and time evolution of the SPP fields, shown in Figures (b)—(f), can then be obtained by collecting electrons having only gained energy via an energy analyzer and reforming the resulting electron images. The figure is taken from Barwick et al. 2009 (reference [45]).

ton processes of the same frequency. For one photon processes energy–momentum conservation is possible in the presence of nanostructures because the nanostructure restores the momentum balance, and the imaging electron can either gain or lose energy in units of the excitation photon energy, $\hbar\omega$. When the electrons that gained energy are selected with an energy filter, the near-fields of nanoscale particles can be imaged with enhanced contrast [45]. This technique is called photoninduced near-field electron microscopy (PINEM). So far the technique has been successful in measuring the near-field patterns of carbon nanotubes, silver nanowires and nanoparticles, and metallic interfaces [45, 46, 103–106]; producing 4-D tomographic maps of a carbon nanotube ring [107]; determining the energy and time correlations, i. e. the chirp, of electron pulses [104]; and demonstrating entanglement of silver nanoparticles through their plasmon fields [108]. The size, polarization, material and spatiotemporal dependence of this near-field imaging are discussed in [44] using Rayleigh and Mie scatterings.

The PINEM arrangement [45] was applied in a recent experiment by Schäfer and Ropers to coherently control the quantum states of free electrons [54]. Following the PINEM setup, electron pulses of 700—900 fs generated by laser emission from a sharp field emission tip were accelerated and focused to a spot size of 15 nm in the optical near-fields of a target addressed with pulsed 800 nm laser light from a Ti:Saph oscillator. The experimental target used was a sharp gold taper, ~100 nm at the apex, etched with a 750 nm periodic grating structure via focused ion beam milling into the side of the taper ~10 μm from the apex [109, 110]. The periodicity of the structure is chosen to couple strongly to the 800 nm laser light in order to generate surface plasmons on the edge of the taper, which can be channeled down the length of the taper. In contrast to previous PINEM experiments, the target 800 nm laser pulses were stretched by dispersion in glass to 3.4 ps so that the plasmonic excitations generated on the taper surface lasted much longer than the duration of the passing electron pulses. The resulting electron energy spectra demonstrated oscillations among the central zero-loss peak and photon sidebands as a function of the laser driving field intensity, thus directly evidencing multilevel Rabi oscillations in the electron energy states. Theoretical support was provided to suggest that the femto-second electron pulses interacting with the nanostructure are transformed into trains of attosecond pulses. This is an interesting alternative to the first all-optical proposal to create atto-second pulses [37].

Finally, PINEM has been used to image biological specimens with femto-second (fs) temporal and nanoscale spatial resolution. This method was demonstrated in imaging of protein vesicles and whole cells of *Escherichia coli* [111].

8. Micro manipulation on a chip

An electron with a velocity of v =3.8 × 10^7 m/s (4 keV) passing over a nano-fabricated grating with a d = 100 nm periodicity, passes adjacent bars in a time of 2.7 fs. This time matches the period of a λ = 800 nm laser closely, and thus gives the possibility of manipulating electron motion with the evanescent fields excited by a laser focussed on the grating, as the grating

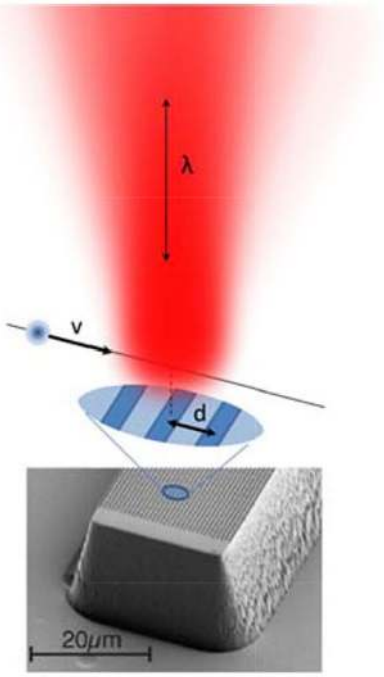

Figure 10. Laser-based microaccelerator. An electron that passes over a grating that is illuminated by a laser beam can be accelerated by the laser beam's electric field. As the travel time, d/v, is matched by the laser period times the excitation order, $n\lambda/c$, the symmetry of the oscillating field is broken and the grating acts as a force rectifier. The figure is modified from Breuer & Hommelhoff 2013 (reference [2]).

can act as a rectifier (Fig. 10). This technique of using nano-fabricated gratings in conjunction with ultrashort laser pulses for particle accelerationwas first proposed by Byer et. al. [112] In comparison, the KD-effect is not due to the electric field of the laser directly but due to the time-averaged Lorentz force (or the ponderomotive potential), and is thus a weaker effect. Accelerations of 20 MeV/m have been reached for incident electron energies of 27.7 keV for a 20 micron length accelerator that pass 50 nm away from the surface of a grating with a 750 nm periodicity at a laser wavelength of 787 nm [2]. Note that the third spatial mode, $n = 3$, was excited on the grating.

The promising feature of micro accelerators is that the maximum accelerating field in conventional linear accelerators is limited to the surface breakdown of the RF cavities at 200 MV/m, while the damage threshold of the gratings lies at much higher fields of 30 GV/m. How these large fields can be used to make small accelerators appears to be a coming technological development. Matching such accelerators to electron beam devices and applying them to accelerate electron beams of a size that is larger than just nanometers are a couple of the obstacles that need to be overcome. Nevertheless, current applications of micro accelerators may be found in novel X-ray sources [113], ultrafast control of electron waves as needed for ultrafast electron diffraction, and particle accelerators for medical applications such as cancer treatment [2, 3]. Additionally, proposals for 2D structures [2] and 3D structures [114] may be realized to enhance the number of electrons that are accelerated providing other effects such as electron beam confinement.

Accelerations beyond 250 MeV/m have been reported for relativistic electrons using micro-fabricated dielectric laser accelerators, which use fused silica grating structures [57]. This is the first demonstration of a scalable laser-driven acceleration system. Multi-stage dielectric laser accelerators based on this result may lead to table-top accelerators on the MeV to GeV scale.

9. Interaction free measurement

Measurement can affect the quantum evolution of a system. A postulate of quantum mechanics is that upon a certain measurent of an observable the wavefunction collapses into the eigenstate of the operator associated with the observable. Less often used is that non-measurement can also affect the quantum evolution. This has a long history going back to Mott's 1929 problem [115] of how to describe tracks in bubble chambers, Renninger's 1960 investigation [116] on howthe non-observation of a radioactive decay in a hemi-sphere is decribed, and a beautiful thought experiment by Elitzur and Vaidman [117] on how to detect a bomb with light that is triggered by a single photon. This may appear impossible, but was demonstrated by Paul Kwiat [118]. The idea is to split a little bit (with probability $P = t/\tau$, where t is the interaction time and $1/\tau$ is the transition rate) from an intial single state into a superposition of two states, and repeat for N cycles. After one cycle the survival probability of the original state will be $P^{(1)}(t) = 1 - t/\tau$ in a classical description. However splitting a little bit of the amplitude and using the Born rule gives $P^{(1)} = 1 - (t/\tau)^2$, in a quantum description. After N cycles the survival probability is given by $P^{(N)}(t) = \{P^{(1)}(t/N)\}^N$. Using the classical probability gives

$$P^{(N)}(t) = \left(1 - (t/N\tau)\right)^N \rightarrow 1 - t/\tau \tag{5}$$

For the quantum case, the survival probability after N cycles is given by

$$P^{(N)}(t) = \left(1 - (t/N\tau)^2\right)^N \rightarrow 1 \tag{6}$$

The non-observation of many weak interactions freezes the evolution into the original state. This is a version of the quantum Zeno effect.

This idea is used in interaction free measurement and in the "Quantum Electron Microscope" (QEM) version of it. In the QEM [20, 21] an electron is coupled into a recycling cavity (Fig. 11). In the cavity the electron wave is diffracted from a standing wave of light in the Bragg regime [119], so that only two beams emerge. The laser light intensity is chosen so that after one cycle only a little bit of electron amplitude contributes to the scattered electron wave. An object consisting out of dark and bright pixels is placed into the weakly scattered electron beam. If the object is positioned so that the dark pixel is in the beam, the electron cannot scatter to this beam and is not observed there. The quantum Zeno effect keeps the electron in

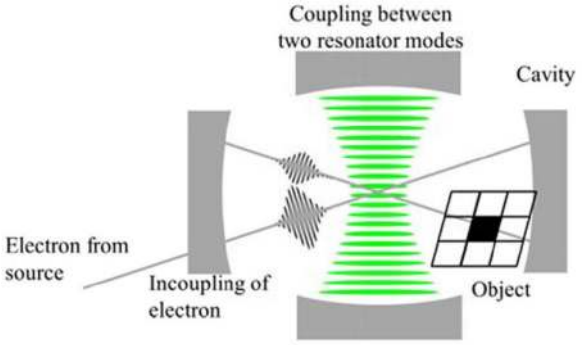

Figure 11. Interaction-free measurement. The presence of a dark pixel in the image of an object can be detected without exposing it by electrons. The ultimate goal of the development of this technique is to be able to probe, with electron microscopes, samples that would otherwise be affected by electron exposure. For explanation see text. (Figure courtesy of Thomas Juffmann at Stanford).

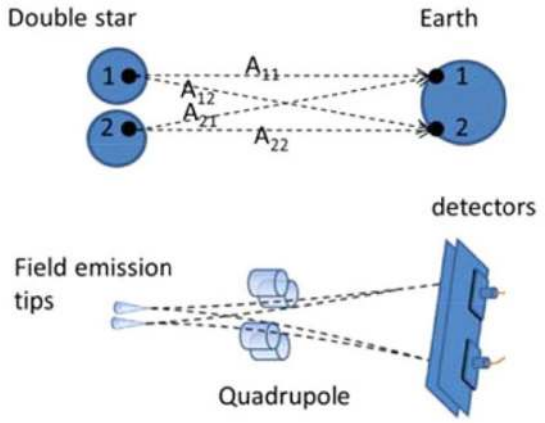

Figure 12. Hanbury Brown Twiss effect analogue. (Top) Correlations are measured on Earth between two separate detectors for photons coming from two separate stars. (Bottom) A schematic of a proposed electron matter wave analogue is shown.

the original unscattered wave (Eq. (6)). If there is a bright pixel in the scattered electron beam the evolution is not affected and after a certain high number of cycles the electron is completely scattered. If the electron is found in the unscattered beam the pixel is dark, if it is not found the pixel is bright.

Now how much exposure did the dark pixel get? The scattering probability, which would direct the electron onto the dark pixel and expose it, is one minus the survival probability or $1 - P^{(N)}(t) \rightarrow 0$. Thus there is no exposure. If a classical description is given, the exposure would be $1 - P^{(N)}(t) \rightarrow t/\tau$ — and large. Hence the name quantum electron microscope. The issues of how does this work for grey pixels and can the cycle time be much longer than the decoherence time are being investigated. The dream of observing biological and even living specimens may be realized in this fashion.

10. Degenerate electron quantum optics

In atomic structure, materials properties, and even astronomical objects, degeneracy and the Pauli Exclusion Principle (PEP) play a major role. The periodic table for atoms, compressibility of solids, and the stability of white dwarfs are examples of this [120]. For free electrons there appears to be only one example where the PEP matters. In 2002, a quantum optics effect was reported for free electrons [22]. Electrons were continuously emitted from a field emission tip and propagated in free space to a detector that was split into two parts and both parts were placed at the same distance from the tip. It was observed that electrons have a tendency not to arrive at the same time at the detectors. This antibunching effect, attributed to the PEP and in close analogy to its earlier photonic analogy, is an example of the Hanbury-Brown Twiss effect. Hanbury-Brown and Twiss (HBT) proved their theory [121, 122], by giving accurate measures of the angular size of several stars using radio and optical interferometry. This stimulated discussion on the nature of light. The classical wave derivation of the HBT effect is straightforward, but the explanation using the second quantized particle description of light, is not. How can two photons measured on Earth on separate detectors be correlated when each originated from a different star (Fig. 12)? The answer to this question was given only after a few years by the Nobel laureate Roy Glauber [123], an answer that marked the birth of the field of Quantum Optics. In the simplest derivation of the HBT effect two sources and two detectors are considered. The intensity correlation between the two detectors is shown to exhibit interference between two amplitudes associated with twoparticle detection. The interfering two-particle amplitudes are A_{11+22} and A_{12+21}, where the first index in the pair "ij" indicates the source and second indicates the detector (Fig. 12). The essential new element is that two-particle amplitudes interfere with eachother.

The observation of the HBT for electrons, immediately raises the question if effects, such as heralded photons [124], the Hong-Ou-Mandel effect [125] and quantum teleportation [126–128], developed in quantum optics for light, can now be explored with electrons. Electron beams are widely used for measuring cross sections, diffraction and microscopy, but these are all one-electron techniques.What would a degenerate two- or more-electron beam add to this? Is such a beam even possible? These are open questions. The purpose of this section is to point out that it is anticipated that high degeneracy two-electron pulses will likely be available in the near future. For the unique antibunching experiment mentioned above, the quantum degeneracy was limited to 10^{-4}. The main reason is that the source was a sharp metal tip placed at a DC voltage. Switching this to laser-field emission at a femto-second scale compresses the electrons to a much smaller time window which can increase the degeneracy by orders of magnitude.

The number of electrons in the coherence volume is called the degeneracy δ. The coherence volume can be thought of as a cylindrical volume. The radial size of the volume is the transverse coherence length, l_t, and the length of the cylinder is the longitudinal coherence length, l_c. The

longitudinal coherence length is related to the coherence time, *tc*. Two electrons are temporally coherent if the time difference in their emission is within the temporal uncertainty of the source. The temporal uncertainty can be found from $\Delta t\,\Delta E \approx \hbar$. The coherence time is $t_c \approx \Delta t \approx \hbar/\Delta E$. If the electrons are traveling at velocity v, then the longitudinal coherence length is $l_c = vt_c \approx v\hbar/\Delta E$. The transverse coherence length, l_t, is dependent on the detected momenta, or in other words, the electron acceptance angle α (Fig. 2). The uncertainty relation gives $l_t \approx \Delta x \approx \hbar/\Delta p \approx \hbar/\alpha p$. Using the de Broglie wavelength gives $l_t \approx \lambda/2\pi\alpha$. Thus the coherence volume is

$$Vc = A_c l_c = (\pi l_t^{\,2})\, l_c \approx \left(\pi\left(\frac{\lambda}{2\pi\alpha}\right)^2\right)\left(\frac{v\hbar}{\Delta E}\right) = \frac{\lambda^2 v\hbar}{4\pi\alpha^2\Delta E} \tag{7}$$

where $A_c = \pi l_t^{\,2}$ is the cross sectional area of the coherence cylinder.

To find the degeneracy, the number of electrons per unit volume from the source must be found. The product of the electrons per volume and the coherence volume gives the number of electrons in the coherence volume. The crosssectional area of the volume is the cross-sectional area of the tip surface, which has a diameter of d_{tip}. The longitudinal length of the volume is determined from the electron packet's temporal width, Δt_p by, $l = v\Delta t_p$. The degeneracy follows as

$$\delta \approx \frac{N}{\pi\left(\frac{d_{\text{tip}}}{2}\right)^2 v\Delta t_p} V_c \tag{8}$$

where N is the number of electrons per pulse and in the last step $l_c = vt_c$ is used. In terms of the current density, $j \equiv Nq/(\pi r^2 \Delta t_p)$, where q is the charge of an electron, the degeneracy is $\delta \approx (j/q)\, A_c t_c$ [129]. In terms of experimental parameters,

$$\delta \approx \frac{N}{\pi\left(\frac{d_{\text{tip}}}{2}\right)^2 \Delta t_p}\;\frac{\lambda^2\hbar}{4\pi\alpha^2\Delta E} = \frac{Nh^3L^2}{\pi^3 m d^2 d_{\text{tip}}^{\,2}\, E\,\Delta E\,\Delta t_p} \tag{9}$$

where $E = mv^2/2$ and the de Broglie wavelength has been used, and the divergence angle is about $\alpha = d/2L$, where d is the diameter of the pinhole (Fig. 13).

From Eq. (9) and the parameters of the system, the degeneracy can be calculated. Tips have a typical diameter of about 50 nm. The D.C. voltage range on the tip is E = 400 eV with a width of ΔE = 0.8 eV [34]. An average of ten electrons per laser pulse, N = 10 was observed [130]. The detector can be placed L = 1 cm from the tip with a pinhole of 5 μm. For a pulse duration of 100 fs. A degeneracy of $\delta \sim 1$ results from these parameters. Upon propagation the Coulomb interaction and degeneracy have been shown to give comparable modification for the joint probability as measured on a split detector [19]. The signal at the detector pinhole would $N_{\text{det}} \approx Nd^2/D^2 \approx 10^{-6}$ per pulse or 10^2 per second. It should be noted that the degeneracy is not available at the detector but only the consequences of the degeneracy at the tip are measurable at the detector. Nevertheless the use of lenses for tranverse refocussing and a dispersion compensator for longitudinal compression give rise to the possibility to deliver a two-electron degenerate pulse on a target.

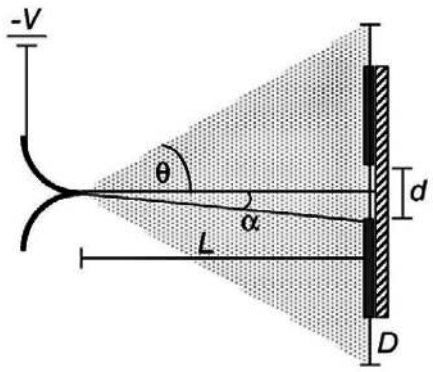

Figure 13. System Schematic. A femto-second laser focused on the tip of a field-emission tip with a DC voltage of $-V$ causes electron emission from the tip. The electrons are selected within an angle of α by a pinhole with diameter d that is located a distance L from the tip. At the detector plane, the electron beam width D is set by the ejection angle θ.

11. Outlook

In the introduction several questions were asked. How much radiation damage do low energy resonances impart to humans? [1] Leon Sanche showed that low-energy electrons can break strands in DNA, [1] and can cause mutations or cancer. The standard practice of ignoring the low-energy electron dosage is thus possibly not sound. The answer to the question on radiation damage depends on identifying very narrow low-energy negative ion resonances. These resonances have not yet been resolved in energy, nor have their total cross sections been measured. Thus their contribution to radiation damage is unknown. It is clear that some of these resonances are strongly present in low-energy electron scattering experiments and should thus not be ignored. The approach of using continuous electron beams and monochromators may lead to answers [131–133]. Alternatively, and not explored as of yet, a femto-second electron time-of-flight apparatus consisting of a pulsed source, dispersion compensator, and fast detector may provide the energy resolution to resolve and measure the cross section of such resonances.

Can charged particle radiation therapy be made more cost-effective? [2,3] Currently $100M accelerators are used at hospital for radiation therapy. If micro-accelerators can be made to work with sufficient current and energy, charged particle radiation may become much more widely available at lower cost. This is

by no means an easy task. The new development, that small surface structures illuminated by laser beams can accelerate electrons by signififfcant amounts, is promising. Challenges will be to accelerate other charged particles (protons) and change the small structures to accomodate acceleration of larger currents of charged particles.

How will movies of protein folding and other biological processes be made? [4,5]. One possible answer is, by using one shot multi-electron ultrafast electron diffraction, so that dynamical effects of damage by electron exposure happens after the image is taken. To overcome dispersion or compensate for Coulomb repulsion, some of the techniques such as RF compression and dispersion compensation may be used to achieve this goal. Another answer is by interaction free electron microscopy which avoids electron exposure altogether.

Can the electron trajectory in a double-slit experiment be tracked? The photon version of this experiment has been realized in 2011, [6] in an application of quantum weak measurement, and leading to much discussion on the meaning of complementarity. The matter wave version is now natural to contemplate and may require single electron sources, control of polarization, direction, and strength of interaction such as can be provided by laser interaction with free coherent electrons.

Can the coupling between gravity and electromagnetism be observed? [7–9] This depends on being able to observe free fall of electrons [7]. Earlier attempts at this were inconclusive [8] and were done with microsecond electron pulses. The problem is that electrons are light and strongly respond to electromagnetic fields. This means that only fairly fast electron pulses have ever been made. To observe the very small change in velocity that gravity makes on an electron in a laboratory, high temporal resolution of electron flightimes are needed. Femto-second electron pulses and detectors may provide a way to perform conclusive experiments.

Is the Pauli exclusion principle (PEP) a symmetry or a consequence of dynamics? [10, 11] Experiments that test for the presence of states that violate PEP have put very stringent limits on their existence [134]. The situation for the dynamical onset of the PEP is much less investigated. Electron scattering from atoms at 10^{-15} s timescales has been proposed to test this [10]. Alternatively, two degenerate electrons, produced at fast timescales available from atto-second laser driven field emission tips may be used to shed light on this question. As the coherence volume of electrons emitted from a nanotip is roughly $(1\ \mu m)^3$, it takes light 3 femto-seconds to cross the coherence volume. If both electrons are produced in less than a femto-second then there is not enough time to signal the presence of the first electron, not even with the speed of light.Will the second electron "know" that the first one is there and obey the PEP? Or, in other words, can the non-locality of PEP be demonstrated?

In summary, new technologies are being developed to manipulate free electrons with laser light and in the vicinity of nano-structures that may have wide implications for technology and fundamental studies.

Acknowledgments — The authors acknowledge helpful discussions with Brett Barwick, Shawn Hilbert, Pieter Kruit, Ben McMorran, and Ahmed Zewail. This work is supported by the National Science Foundation under Grant No. 1306565. This work is part of the research program of the Foundation for Fundamental Research on Matter (FOM), which is part of the Netherlands Organization for Scientific Research (NWO).

Eric Jones studied physics at the University of New York at Stony Brook and is a graduate student at the University of Nebraska–Lincoln working on electron matter waves, femto-second lasers and nanowires.

Maria Becker studied physics at the University of Nebraska–Lincoln and the University of Texas-Austin and is a graduate student at the University of Nebraska-Lincoln working on electron matter waves, femto-second lasers, and plasmonic antennas.

Jom Luiten obtained his PhD in 1993 at the University of Amsterdam. After working for several years on superconducting X-ray detectors and spending a year in industry he turned to accelerator and beam physics at Eindhoven University of Technology (TU/e) in 1998. Currently he is heading the TU/e group Coherence and Quantum Technology, conducting research on coherent charged particle beams, ultracold plasmas, ultrafast electron diffraction and microscopy, and coherent light-matter interaction.

Herman Batelaan studied physics at the University of Leiden and obtained the Ph.D. at the University of Utrecht. After temporary positions at the State University of New York at Stony Brook, Universität Innsbruck, University of Nebraska–Lincoln and the Technische Universiteit Eindhoven, he became a professor at the University of Nebraska–Lincoln. He is a fellow of the American Physical Society for "outstanding contributions to electron matter optics, in particular the measurements of the Kapitza-Dirac effect and elucidation of the Aharonov-Bohm effect."

References

[1] B. Boudaïffa, P. Cloutier, D. Hunting, M. A. Huels, and L. Sanche, Science **287**, 1658–1660 (2000).

[2] J. Breuer and P. Hommelhoff, Phys. Rev. Lett. **111**, 134803 (2013).

[3] D. Orf, Pop. Mech., http://www.popularmechanics.com/how-to/blog/cheaper-micro-sized-particle-accelerators-are- now-possible-15987492 (14 August 2015).

[4] K. A. Dill and J. L. MacCallum, Science **338**, 1042–1046 (2012).

[5] R. J. D. Miller, R. Ernstorfer, M. Harb, M. Gao, C. T. Hebeisen, H. Jean-Ruel, C. Lu, G. Moriena, and G. Sciaini, Acta Crystallogr. A **66**, 137–156 (2010).

[6] S. Kocsis, B. Braverman, S. Ravets, M. J. Stevens, R. P. Mirin, L. K. Shalm, and A. M. Steinberg, Science **332**, 1170–1173 (2011).

[7] F. C. Witteborn and W. M. Fairbank, Nature **220**, 436–440 (1968).

[8] T. W. Darling, F. Rossi, G. I. Opat, and G. F. Moorhead, Rev. Mod. Phys. **64**, 237–257 (1992).

[9] M. Becker, A. Caprez, and H. Batelaan, Atoms **3**, 320–338 (2015).

[10] A. Shimony, Quantum Inf. Process. **5**, 277–286 (2006).

[11] S. R. Elliott, B. H. LaRoque, V. M. Gehman, M. F. Kidd, and M. Chen, Found. Phys. **42**, 1015–1030 (2012).

[12] D. L. Freimund, K. Aflatooni, and H. Batelaan, Nature **413**, 142–143 (2001).

[13] P. Hommelhoff, Y. Sortais, A. Aghajani-Talesh, and M. A. Kasevich, Phys. Rev. Lett. **96**, 077401 (2006).

[14] B. Barwick, C. Corder, J. Strohaber, N. Chandler-Smith, C. Uiterwaal, and H. Batelaan, New J. Phys. **9**, 142 (2007).

[15] M. Krüger, M. Schenk, and P. Hommelhoff, Nature **475**, 78–81 (2011).

[16] S. A. Hilbert, C. Uiterwaal, B. Barwick, H. Batelaan, and A. H. Zewail, Proc. Natl. Acad. Sci. **106**, 10558–10563 (2009).

[17] M. Becker, W. C.-W. Huang, H. Batelaan, E. J. Smythe, and F. Capasso, Ann. Phys. **525**, L6–L11 (2013).

[18] J. Hammer, S. Thomas, P.Weber, and P. Hommelhoff, Phys. Rev. Lett. **114**, 254801 (2015).

[19] P. Lougovski and H. Batelaan, Phys. Rev. A **84**, 023417 (2011).

[20] W. P. Putnam and M. F. Yanik, Phys. Rev. A **80**, 040902 (2009).

[21] http://www.rle.mit.edu/qem/ (12 August 2015).

[22] H. Kiesel, A. Renz, and F. Hasselbach, Nature **418**, 392–394 (2002).

[23] P. L. Kapitza and P. a. M. Dirac, Math. Proc. Camb. Philos. Soc. **29**, 297–300 (1933).

[24] P. H. Bucksbaum, M. Bashkansky, and T. J. McIlrath, Phys. Rev. Lett. **58**, 349–352 (1987).

[25] http://www.nobelprize.org/nobel_prizes/physics/laureates/1997/ (12 August 2015).

[26] G. Gronniger, B. Barwick, H. Batelaan, T. Savas, D. Pritchard, and A. Cronin, Appl. Phys. Lett. **87**, 124104 (2005).

[27] R. Bach, D. Pope, S.-H. Liou, and H. Batelaan, New J. Phys. **15**, 033018 (2013).

[28] M. Uchida and A. Tonomura, Nature **464**, 737–739 (2010).

[29] B. J. McMorran, A. Agrawal, I. M. Anderson, A. A. Herzing, H. J. Lezec, J. J. McClelland, and J. Unguris, Science **331**, 192–195 (2011).

[30] G. Gronniger, B. Barwick, and H. Batelaan, New J. Phys. **8**, 224 (2006).

[31] A. D. Cronin and B. McMorran, Phys. Rev. A **74**, 061602 (2006).

[32] B. J. McMorran and A. D. Cronin, New J. Phys. **11**, 033021 (2009).

[33] R. Bach, G. Gronniger, and H. Batelaan, Appl. Phys. Lett. **103**, 254102 (2013).

[34] S. A. Hilbert, B. Barwick, M. Fabrikant, C. J. G. J. Uiterwaal, and H. Batelaan, Appl. Phys. Lett. **91**, 173506 (2007).

[35] T. van Oudheusden, E. F. de Jong, S. B. van der Geer, W. P. E. M. Op 't Root, O. J. Luiten, and B. J. Siwick, J. Appl. Phys. **102**, 093501 (2007).

[36] T. van Oudheusden, P. L. E. M. Pasmans, S. B. van der Geer, M. J. de Loos, M. J. van der Wiel, and O. J. Luiten, Phys. Rev. Lett. **105**, 264801 (2010).

[37] P. Baum and A. H. Zewail, Proc. Natl. Acad. Sci. **104**, 18409–18414 (2007).

[38] P. Hansen, C. Baumgarten, H. Batelaan, and M. Centurion, Appl. Phys. Lett. **101**, 083501 (2012).

[39] W. J. Engelen, M. A. van der Heijden, D. J. Bakker, E. J. D. Vredenbregt, and O. J. Luiten, Nat. Commun. **4**, 1693 (2013).

[40] R. D. Young and E. W. Müller, Phys. Rev. **113**, 115–120 (1959).

[41] A. Tonomura, Electron Holography, 2nd, enlarged ed. 1999 edition (Springer, Berlin, New York, 1999).

[42] B. Cho, T. Ichimura, R. Shimizu, and C. Oshima, Phys. Rev. Lett. **92**, 246103 (2004).

[43] D. Ehberger, J. Hammer, M. Eisele, M. Krüger, J. Noe, A. Högele, and P. Hommelhoff, Phys. Rev. Lett. **114**, 227601 (2015).

[44] S. T. Park, M. Lin, and A. H. Zewail, New J. Phys. **12**, 123028 (2010).

[45] B. Barwick, D. J. Flannigan, and A. H. Zewail, Nature **462**, 902–906 (2009).

[46] L. Piazza, T. T. A. Lummen, E. Quiñonez, Y. Murooka, B. W. Reed, B. Barwick, and F. Carbone, Nat. Commun. **6** (2015).

[47] A. H. Zewail, Annu. Rev. Phys. Chem. **57**, 65–103 (2006).

[48] B. J. Siwick, J. R. Dwyer, R. E. Jordan, and R. J. D.Miller, Science **302**, 1382–1385 (2003).

[49] M. Gulde, S. Schweda, G. Storeck, M. Maiti, H. K. Yu, A. M. Wodtke, S. Schäfer, and C. Ropers, Science **345**, 200–204 (2014).

[50] E. T. J. Nibbering, Science **345**, 137–138 (2014).

[51] T. LaGrange, M. R. Armstrong, K. Boyden, C. G. Brown, G. H. Campbell, J. D. Colvin, W. J. DeHope, A. M. Frank, D. J. Gibson, F. V. Hartemann, J. S. Kim, W. E. King, B. J. Pyke, B. W. Reed, M. D. Shirk, R. M. Shuttlesworth, B. C. Stuart,

B. R. Torralva, and N. D. Browning, Appl. Phys. Lett. **89**, 044105 (2006).

[52] J. S. Kim, T. LaGrange, B. W. Reed, M. L. Taheri, M. R. Armstrong, W. E. King, N. D. Browning, and G. H. Campbell, Science **321**, 1472–1475 (2008).

[53] B. W. Reed, M. R. Armstrong, N. D. Browning, G. H. Campbell, J. E. Evans, T. LaGrange, and D. J. Masiel, Microsc. Microanal. Off. J. Microsc. Soc. Am. Microbeam Anal. Soc. Microsc. Soc. Can. **15**, 272–281 (2009).

[54] A. Feist, K. E. Echternkamp, J. Schauss, S. V. Yalunin, S. Schäfer, and C. Ropers, Nature **521**, 200–203 (2015).

[55] A. Lassise, P. H. A. Mutsaers, and O. J. Luiten, Rev. Sci. Instrum. **83**, 043705 (2012).

[56] E. J. Smythe, E. Cubukcu, and F. Capasso, Opt. Express **15**, 7439–7447 (2007).

[57] E. A. Peralta, K. Soong, R. J. England, E. R. Colby, Z.Wu, B. Montazeri, C. McGuinness, J. McNeur, K. J. Leedle, D. Walz, E. B. Sozer, B. Cowan, B. Schwartz, G. Travish, and R. L. Byer, Nature **503**, 91–94 (2013).

[58] Y. W. Chan and W. L. Tsui, Phys. Rev. A **20**, 294–303 (1979).

[59] H. Batelaan, Rev. Mod. Phys. **79**, 929–941 (2007).

[60] B. McMorran, J. D. Perreault, T. A. Savas, and A. Cronin, Ultramicroscopy **106**, 356–364 (2006).

[61] R. P. Feynman, R. B. Leighton, and M. S. Sands, The Feynman Lectures on Physics, Vol. 3, Later Printing Used edition (Addison Wesley, 1971).

[62] J. Verbeeck, H. Tian, and P. Schattschneider, Nature **467**, 301–304 (2010).

[63] J. Verbeeck, P. Schattschneider, S. Lazar, M. Stöger- Pollach, S. Löffler, A. Steiger-Thirsfeld, and G. V. Tendeloo, Appl. Phys. Lett. **99**, 203109 (2011).

[64] J. Handali, P. Shakya, and B. Barwick, Opt. Express **23**, 5236 (2015).

[65] S. Fürhapter, A. Jesacher, S. Bernet, and M. Ritsch-Marte, Opt. Lett. **30**, 1953–1955 (2005).

[66] P. Hommelhoff, C. Kealhofer, and M. A. Kasevich, Phys. Rev. Lett. **97**, 247402 (2006).

[67] L. Kasmi, D. Kreier, M. Bradler, E. Riedle, and P. Baum, New J. Phys. **17**, 033008 (2015).

[68] M. Krüger, M. Schenk, M. Förster, and P. Hommelhoff, J. Phys. B At. Mol. Opt. Phys. **45**, 074006 (2012).

[69] C. Ropers, D. R. Solli, C. P. Schulz, C. Lienau, and T. Elsaesser, Phys. Rev. Lett. **98**, 043907 (2007).

[70] G. Herink, D. R. Solli, M. Gulde, and C. Ropers, Nature **483**, 190–193 (2012).

[71] L. Wimmer, G. Herink, D. R. Solli, S. V. Yalunin, K. E. Echternkamp, and C. Ropers, Nat. Phys. **10**, 432–436 (2014).

[72] M. Moshinsky, Phys. Rev. **88**, 625–631 (1952).

[73] Č. Brukner and A. Zeilinger, Phys. Rev. A **56**, 3804–3824 (1997).

[74] G. Muga, A. Ruschhaupt, and A. Campo, Eds., Time in Quantum Mechanics II (Springer, Berlin & Heidelberg, 2009).

[75] M. Beau and T. C. Dorlas, Int. J. Theor. Phys. **54**, 1882–1907 (2014).

[76] P. Szriftgiser, D. Guéry-Odelin, M. Arndt, and J. Dalibard, Phys. Rev. Lett. **77**, 4–7 (1996).

[77] T. Hils, J. Felber, R. Gähler, W. Gläser, R. Golub, K. Habicht, and P. Wille, Phys. Rev. A **58**, 4784–4790 (1998).

[78] F. Lindner, M. G. Schätzel, H. Walther, A. Baltuška, E. Goulielmakis, F. Krausz, D. B. Milošević, D. Bauer, W. Becker, and G. G. Paulus, Phys. Rev. Lett. **95**, 040401 (2005).

[79] R. P. Chatelain, V. R. Morrison, C. Godbout, and B. J. Siwick, Appl. Phys. Lett. **101**, 081901 (2012).

[80] V. R. M. Robert P. Chatelain, Appl. Phys. Lett. **101** (2012).

[81] J. Luiten, Europhys. News **46**, 21–25 (2015).

[82] K. P. Grzelakowski and R. M. Tromp, Ultramicroscopy **130**, 36–43 (2013).

[83] K. P. Grzelakowski, Ultramicroscopy **116**, 95–105 (2012).

[84] K. P. Grzelakowski, Ultramicroscopy **130**, 29–35 (2013).

[85] M. Gao, Y. Jiang, G. Kassier, and R. J. D. Miller, Appl. Phys. Lett. **103** (2013).

[86] W. C.-W. Huang, R. Bach, P. Beierle, and H. Batelaan, J. Phys. Appl. Phys. **47**, 085102 (2014).

[87] C. T. Hebeisen, G. Sciaini, M. Harb, R. Ernstorfer, T. Dartigalongue, S. G. Kruglik, and R. J. D. Miller, Opt. Express **16**, 3334 (2008).

[88] V. S. Yakovlev, M. I. Stockman, F. Krausz, and P. Baum, Sci. Rep. **5**, 14581 (2015).

[89] H.-C. Shao and A. F. Starace, Phys. Rev. Lett. **105**, 263201 (2010).

[90] D. J. Flannigan and A. H. Zewail, Acc. Chem. Res. **45**, 1828–1839 (2012).

[91] G. Sciaini and R. J. D. Miller, Rep. Prog. Phys. **74**, 096101 (2011).

[92] D. Shorokhov and A. H. Zewail, Phys. Chem. Chem. Phys. **10**, 2879–2893 (2008).

[93] M. Chergui and A. H. Zewail, ChemPhysChem **10**, 28–43 (2009).

[94] F. O. Kirchner, A. Gliserin, F. Krausz, and P. Baum, Nat. Photonics **8**, 52–57 (2014).

[95] O. Muskens, Ann. Phys. **525**, A21–A22 (2013).

[96] A. H. Zewail, J. Phys. Chem. A **104**, 5660–5694 (2000).

[97] T. Plettner, R. L. Byer, C. McGuinness, and P. Hommelhoff, Phys. Rev. Spec. Top. - Accel. Beams **12**, 101302 (2009).

[98] L. O'Faolain, D. M. Beggs, T. P. White, T. Kampfrath, K. Kuipers, and T. F. Krauss, IEEE Photonics J. **2**, 404–414 (2010).

[99] E. Esarey, P. Sprangle, and J. Krall, Phys. Rev. E **52**, 5443–5453 (1995).

[100] F. J. G. de Abajo and M. Kociak, New J. Phys. **10**, 073035 (2008).

[101] F. J. García de Abajo, Rev. Mod. Phys. **82**, 209–275 (2010).

[102] F. J. García de Abajo, A. Asenjo-Garcia, and M. Kociak, Nano Lett. **10**, 1859–1863 (2010).

[103] A. Yurtsever, R. M. van derVeen, and A. H. Zewail, Science **335**, 59–64 (2012).

[104] S. T. Park, O.-H. Kwon, and A. H. Zewail, New J. Phys. **14**, 053046 (2012).

[105] A. Yurtsever and A. H. Zewail, Nano Lett. **12**, 3334–3338 (2012).

[106] L. Piazza, D. J. Masiel, T. LaGrange, B. W. Reed, B. Barwick, and F. Carbone, Chem. Phys. **423**, 79–84 (2013).

[107] O.-H. Kwon and A. H. Zewail, Science **328**, 1668–1673 (2010).

[108] A. Yurtsever, J. S. Baskin, and A. H. Zewail, Nano Lett. **12**, 5027–5032 (2012).

[109] C. Ropers, C. C. Neacsu, T. Elsaesser, M. Albrecht, M. B. Raschke, and C. Lienau, Nano Lett. **7**, 2784–2788 (2007).

[110] C. Ropers, T. Elsaesser, G. Cerullo, M. Zavelani-Rossi, and C. Lienau, New J. Phys. **9**, 397 (2007).

[111] D. J. Flannigan, B. Barwick, and A. H. Zewail, Proc. Natl. Acad. Sci. **107**, 9933–9937 (2010).

[112] T. Plettner, P. P. Lu, and R. L. Byer, Phys. Rev. Spec. Top.-Accel. Beams **9**, 111301 (2006).

[113] B. E. Carlsten, E. R. Colby, E. H. Esarey, M. Hogan, F. X. Kärtner, W. S. Graves, W. P. Leemans, T. Rao, J. B. Rosenzweig, C. B. Schroeder, D. Sutter, and W. E. White, Nucl. Instrum. Methods Phys. Res. Sect. Accel. Spectrometers Detect. Assoc. Equip. **622**, 657–668 (2010).

[114] B. M. Cowan, Phys. Rev. Spec. Top. - Accel. Beams **11**, 011301 (2008).

[115] N. F. Mott, Proc. R. Soc. Lond. Math. Phys. Eng. Sci. **126**, 79–84 (1929).

[116] M. Renninger, Z. Für Phys. **158**, 417–421 (1960).

[117] A. C. Elitzur and L. Vaidman, Found. Phys. **23**, 987–997 (1993).

[118] P. Kwiat, H. Weinfurter, T. Herzog, A. Zeilinger, and M. A. Kasevich, Phys. Rev. Lett. **74**, 4763–4766 (1995).

[119] D. L. Freimund and H. Batelaan, Phys. Rev. Lett. **89**, 283602 (2002).

[120] http://www.wiley.com/WileyCDA/WileyTitle/productCd-0471057002.html (13 August 2015).

[121] R. Hanbury Brown and R. Q. Twiss, Nature **178**, 1046–1048 (1956).

[122] R. H. Brown and R. Q. Twiss, Nature **177**, 27–29 (1956).

[123] R. J. Glauber, Phys. Rev. Lett. **10**, 84–86 (1963).

[124] M. D. Cunha Pereira, F. E. Becerra, B. L. Glebov, J. Fan, S. W. Nam, and A. Migdall, Opt. Lett. **38**, 1609 (2013).

[125] C. K. Hong, Z. Y. Ou, and L. Mandel, Phys. Rev. Lett. **59**, 2044–2046 (1987).

[126] C. H. Bennett, G. Brassard, C. Crépeau, R. Jozsa, A. Peres, and W. K. Wootters, Phys. Rev. Lett. **70**, 1895–1899 (1993).

[127] D. Bouwmeester, J.-W. Pan, K. Mattle, M. Eibl, H. Weinfurter, and A. Zeilinger, Nature **390**, 575–579 (1997).

[128] D. Boschi, S. Branca, F. De Martini, L. Hardy, and S. Popescu, Phys. Rev. Lett. **80**, 1121–1125 (1998).

[129] M. Silverman, More Than One Mystery: Explorations in Quantum Interference, 1995 edition (Springer, New York, 1994).

[130] S. A. Hilbert, A. Neukirch, C. J. G. J. Uiterwaal, and H. Batelaan, J. Phys. B At. Mol. Opt. Phys. **42**, 141001 (2009).

[131] M. C. Fuss, A. G. Sanz, F. Blanco, J. C. Oller, P. Limão-Vieira, M. J. Brunger, and G. García, Phys. Rev. A **88**, 042702 (2013).

[132] J. P. Sullivan, S. J. Gilbert, J. P. Marler, R. G. Greaves, S. J. Buckman, and C. M. Surko, Phys. Rev. A **66**, 042708 (2002).

[133] J. P. Sullivan, A. Jones, P. Caradonna, C. Makochekanwa, and S. J. Buckman, Rev. Sci. Instrum. **79**, 113105 (2008).

[134] E. Ramberg and G. A. Snow, Phys. Lett. B **238**, 438–441 (1990).